Research on Pedestrian Location Based on Dual MIMU/ Magnetometer/ Ultrasonic Module

Wang qiuying, Guo Zheng, Zhang minghui, Cui Xufei*
College of Information and Communication Engineering
Harbin Engineering University
Harbin, China
wangqiuying@hrbeu.edu.cn
Wu hui
Dalian Shipbuilding Industry Offshore Co., Ltd
Dalian, China
Jia Li
Department of Electrical and Computer Engineering
Oakland University
Rochester, USA

***Abstract*—Inertial positioning technology is one of the most important positioning techniques. It is suitable for environments without GPS, lack of radio base stations or have no priori geographic information. The pedestrian location system based on Micro Inertial Measurement Unit (MIMU) is usually integrated in the foot of the pedestrian and using the inertial law to solve the pedestrian's position, velocity and attitude information. What's more, the inertial location system utilizes the Zero Velocity Update (ZUPT) algorithm to suppress their errors. However, ZUPTs cannot effectively decrease pedestrian position errors and heading angle error. So pedestrian's position errors and heading angle error will still accumulate over time. Because the magnetometer can detect earth's magnetic field information and solving the heading angle by it, in this paper, a dual MIMU/ magnetometer/ ultrasonic pedestrian location scheme is proposed. The two MIMUs, two magnetometers and two ultrasonic modules are respectively fixed on the left and right foot of pedestrians, and the output information of magnetometer is used to assist the ZUPT algorithm to calculate the locating information, which suppresses positioning error and heading error. We use two ultrasonic modules to measure the spatial relative position relation of pedestrian's left foot and right foot in real time and construct the second order nonlinear constraint equation. We correct pedestrian position information continually by using this constraints so that to improve the positioning accuracy. To verify this program, in this paper, some experiments have been carried out. We have designed different pedestrian trajectories in certain building. After the experiment we processed and analyzed the offline data from this integrated positioning system. The experimental results show that compared with single MIMU pedestrian location scheme, pedestrian positioning technology based on dual MIMU/ magnetometer/ ultrasonic module has higher positioning accuracy, and the positioning accuracy of this system is better in the longer time, which can meet the requirement of pedestrian positioning where there is no external auxiliary information.

Keywords—Inertial positioning; micro inertial measurement unit ; Magnetometer; Ultrasonic wave; Equality constraint; zero velocity update

I. INTRODUCTION

Pedestrian location technology is playing an increasingly important role in many social aspects such as path navigation, medical emergency, public safety, emergency response and military field. The Global Positioning System (GPS) is being widely used. But in indoor environment, the satellite signal is blocked by walls, and its performance is greatly degraded or even unavailable, which cannot meet the location needs of users in the indoor environment for a long time [1-3]. WiFi positioning is often used in the indoor environment, which can meet the normal pedestrian needs. But WiFi is not available in disaster relief and counter-terrorism assault. However, the independent, fully autonomous inertial positioning technology can be applied to a variety of complex and changeable environments. The MIMU is the core component of the inertial positioning system and installed on the foot of pedestrians. The pedestrian position is calculated as measuring the acceleration and angular velocity of pedestrians' feet in real time, and the positioning error is reduced with ZUPTs [4-8]. There are a lot of different ZUPT algorithms, such as acceleration and angular velocity variance detection, acceleration amplitude detection, N-P criterion and hidden Markov detection method, and they can achieve good positioning effect in the corresponding motion state. ZUPTs can effectively suppress the velocity error and horizontal attitude angle error, thus correcting the position error of pedestrians to a certain extent [9-11]. But the heading error and position error of pedestrians can't be well estimated by ZUPTs [12]. To solve this problem, a dual MIMU/ magnetometer/ ultrasonic integrated navigation system is proposed in this paper. The magnetometer can measure the component of the earth's magnetic field on the three-axis of the carrier. The navigation system can use the component of the earth's magnetic field on the horizontal plane to calculate the direction of the direction of the navigation [13]. The MIMU/ magnetometer integrated navigation scheme can suppress the divergence of heading error. Choosing a good ZUPTs algorithm and adding the angle information calculated by the magnetometer can improve the positioning accuracy of pedestrians in a short time, but still cannot meet the needs of long term navigation [14-16]. However, we notice that there is a physical constraint on the position information between the feet in the course of a pedestrian movement. By using this constraint, we can estimate the position error of the pedestrian [17]. In order to restrain the divergence of position error, the ultrasonic distance measuring module is added in this paper. This paper uses the magnetometer information to assist the ZUPT algorithm to suppress the heading error and the distance information between pedestrians' feet measured by ultrasonic wave to reduce the position error. This integrated navigation system can meet the requirements of many environments because it does not require external information, such as GPS and WiFi. And, more importantly, this integrated navigation technology can meet the needs of long-time pedestrian navigation.

II. SYSTEMS DEFINITION

A. Pedestrian positioning technology based on MIMU

MIMU is the core component of the Inertial Navigation System (INS) and it consists of a three-axis accelerometer and a three-axis gyroscope. It is fixed on the foot of a pedestrian and can measure the acceleration and angular velocity of the foot.

The navigation system uses angular velocity to calculate the transformation matrix $\mathbf{C}_b^n$ of the carrier coordinate system to the navigation coordinate system. Then we can projection the acceleration in the body coordinate system to the navigation coordinate system by $\mathbf{C}_b^n$:

$$\mathbf{f}^n = \mathbf{C}_n^N \mathbf{C}_b^n \left(\mathbf{f}^b + \delta\mathbf{f}^b\right) \tag{1}$$

Then velocity $\mathbf{v}^n$:

$$\mathbf{v}^n = \int \mathbf{f}^n dt \tag{2}$$

Finally position $\mathbf{p}^n$:

$$\mathbf{p}^n = \int \mathbf{v}^n dt \tag{3}$$

In the form (1), $\delta\mathbf{f}^b$ is acceleration error and $\mathbf{C}_n^N$ is a conversion matrix due to gyroscope error.

As shown in form (1), due to the noise of MIMU devices, the location error of system increases with time, which is one of the most important factors that restrict the long navigation of inertial location system.

ZUPT method is an error compensation method for an inertial pedestrian positioning system. The navigation system can detect the motion state of pedestrians in real time. When foot touches the ground, it is considered that the foot is relatively static with the ground, and the relative rest time is called "zero velocity interval". In other words, there should be $\mathbf{v}^n = 0$ in zero velocity interval in theory. But in fact, it's not. ZUPTs use the calculating velocity $\mathbf{v}^n$ in zero velocity interval to estimate the position error, velocity error and attitude error of the pedestrians by Kalman filter, so as to compensate the settlement results of the navigation system.

The states of Kalman filter:

$$\mathbf{x} = \begin{bmatrix} \delta\mathbf{p} & \delta\mathbf{v} & \delta\boldsymbol{\varepsilon} \end{bmatrix} \tag{4}$$

One step state transition matrix:

$$\mathbf{A} = \begin{bmatrix} \mathbf{0}_{3\times3} & \mathbf{I}_{3\times3} & \mathbf{0}_{3\times3} \\ \mathbf{0}_{3\times3} & \mathbf{0}_{3\times3} & [\mathbf{f}\times] \\ \mathbf{0}_{3\times3} & \mathbf{0}_{3\times3} & \mathbf{0}_{3\times3} \end{bmatrix} \tag{5}$$

The observations of Kalman filter:

$$\mathbf{z} = \delta\mathbf{v} \tag{6}$$

Observation matrix:

$$\mathbf{H} = \begin{bmatrix} \mathbf{0}_{3\times3} & \mathbf{I}_{3\times3} & \mathbf{0}_{3\times3} \end{bmatrix} \tag{7}$$

In the form, $\delta\mathbf{p}$ is position error of pedestrian, $\delta\mathbf{v}$ velocity error $\delta\boldsymbol{\varepsilon}$ is attitude error, $\mathbf{I}$ is identity matrix .

We have an observability analysis of this mathematical model construct the matrix $\mathbf{Q}$:

$$\mathbf{Q} = \begin{bmatrix} \mathbf{H} \\ \mathbf{HA} \\ \mathbf{HA}^2 \\ \mathbf{HA}^3 \\ \mathbf{HA}^4 \\ \mathbf{HA}^5 \\ \mathbf{HA}^6 \\ \mathbf{HA}^7 \\ \mathbf{HA}^8 \end{bmatrix} \tag{8}$$

Thus,

$$\text{rank}\mathbf{Q} = \begin{bmatrix} \mathbf{H} \\ \mathbf{HA} \\ \mathbf{HA}^2 \\ \mathbf{HA}^3 \\ \mathbf{HA}^4 \\ \mathbf{HA}^5 \\ \mathbf{HA}^6 \\ \mathbf{HA}^7 \\ \mathbf{HA}^8 \end{bmatrix} = \begin{bmatrix} \mathbf{0}_{3\times3} & \mathbf{I}_{3\times3} & \mathbf{0}_{3\times3} \\ \mathbf{0}_{3\times3} & \mathbf{0}_{3\times3} & [\mathbf{f}\times]_{3\times3} \\ \mathbf{0}_{3\times3} & \mathbf{0}_{3\times3} & \mathbf{0}_{3\times3} \\ \mathbf{0}_{3\times3} & \mathbf{0}_{3\times3} & \mathbf{0}_{3\times3} \\ \mathbf{0}_{3\times3} & \mathbf{0}_{3\times3} & \mathbf{0}_{3\times3} \\ \mathbf{0}_{3\times3} & \mathbf{0}_{3\times3} & \mathbf{0}_{3\times3} \\ \mathbf{0}_{3\times3} & \mathbf{0}_{3\times3} & \mathbf{0}_{3\times3} \\ \mathbf{0}_{3\times3} & \mathbf{0}_{3\times3} & \mathbf{0}_{3\times3} \\ \mathbf{0}_{3\times3} & \mathbf{0}_{3\times3} & \mathbf{0}_{3\times3} \end{bmatrix} \tag{9}$$

In the form, $[\mathbf{f}\times]_{3\times3} = \begin{bmatrix} 0 & -\mathrm{f}_z^b & \mathrm{f}_y^b \\ \mathrm{f}_z^b & 0 & -\mathrm{f}_x^b \\ -\mathrm{f}_y^b & \mathrm{f}_x^b & 0 \end{bmatrix}$, and $\mathbf{f}_x^b$, $\mathbf{f}_y^b$, $\mathbf{f}_z^b$ is the output value of the three axis accelerometer. When the foot touches the ground, it is $[\mathbf{f}\times]_{3\times3} = \begin{bmatrix} 0 & -g & 0 \\ g & 0 & 0 \\ 0 & 0 & 0 \end{bmatrix}$. This shows that $\text{rank}\mathbf{Q} = 5$.

That shows that the state of the system is not completely observable. Through our analysis, the pedestrian speed error and two horizontal attitude angle error can be observed, but the position error and heading error of pedestrians are unobservable.

ZUPTS can suppress the system positioning error to a certain extent. But because of the unobservable location error and heading error during the Kalman filtering process, it cannot meet the needs of pedestrian location.

B. Pedestrian positioning technology based on MIMU/ magnetometer/ ultrasonic module

In this paper, the magnetometer is used to correct the heading information of pedestrians. In the process of pedestrian movement, the system can calculate the horizontal attitude angles θ and γ of the carrier in real time. Using the horizontal attitude angle, the magnetometer measurements under the carrier system are projected to the navigation coordinate system, and the measurement values of the magnetometer B^n under the navigation system are obtained:

$$\mathbf{B}^n = \begin{bmatrix} \cos\theta & 0 & -\sin\theta \\ 0 & 1 & 0 \\ -\sin\theta & 0 & \cos\theta \end{bmatrix} \cdot \begin{bmatrix} 1 & 0 & 0 \\ 0 & \cos\gamma & -\sin\gamma \\ 0 & \sin\gamma & \cos\gamma \end{bmatrix} \cdot \mathbf{B}^b \quad (10)$$

In the form, B^b and B^n are the magnetic field intensity of the carrier system and the navigation system respectively. θ and γ are the pitch angle and the roll angle respectively.

Thus the heading angle can be obtained:

$$\phi = \arctan\left(\frac{B_y^n}{B_x^n}\right) + M_d \quad (11)$$

In the form, B_x^n , B_y^n are magnetic field intensity component of x, y axis respectively in the navigation coordinate system. M_d is local declination

The system error is estimated by Kalman filter.

Then we establish the mathematical model:

$$\delta\dot{\mathbf{p}} = \delta\mathbf{v} \quad (12)$$

$$\delta\dot{\mathbf{v}} = -2C_b^n(\hat{q})[f^b\times]\delta\mathbf{q} \quad (13)$$

$$\delta\dot{\mathbf{q}} = -[\hat{\boldsymbol{\omega}}_b\times]\delta\mathbf{q} - \frac{1}{2}\delta\mathbf{q} \quad (14)$$

In the form, $\delta\mathbf{p}$ is position error of pedestrian, $\delta\mathbf{v}$ velocity error, $\delta\mathbf{q}$ is quaternion error.

The states of Kalman filter:

$$\mathbf{x} = [\delta\mathbf{p} \quad \delta\mathbf{v} \quad \delta\mathbf{q} \quad \mathbf{b}_a \quad \mathbf{b}_w] \quad (15)$$

The observations of Kalman filter:

$$\mathbf{z} = [\delta\mathbf{v} \quad \delta\mathbf{q}] \quad (16)$$

The heading information of the magnetometer is added to each ZUPT, which greatly improves the observability of the heading angle of pedestrian.

In order to correct the position information of pedestrians effectively, this paper uses the integrated navigation system based on dual MIMU/ Magnetometer/ Ultrasonic module. On the left and right foot of the pedestrians, inertial measurement elements, magnetometers and ultrasonic modules are installed respectively. The ultrasonic module can measure the distance $\vartriangle R$ between pedestrians in real time.

Generally, in the course of walking, one foot is touchable, while the other is away from the ground. In this paper, the right foot touches the bottom and the left foot is out of the ground as an example. Figure1 is a sketch map of pedestrians' feet at the certain moment. The dotted line indicates the distance between two feet measured by the ultrasonic distance measuring module and the distance is $\vartriangle R$. The real line represents the true track of the left foot movement. The dash dot indicates the incorrect trajectory due to system noise.

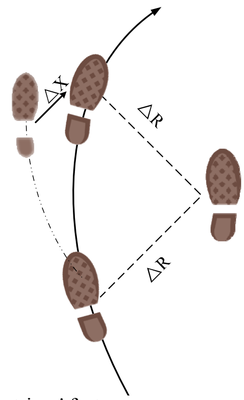

Fig.1 Sketch map of pedestrians' feet

The integrated navigation system uses ZUPT algorithm to calculate right foot's position, speed and attitude aided by magnetometer. At the same time, the position information of the other foot is corrected by the distance between two feet.

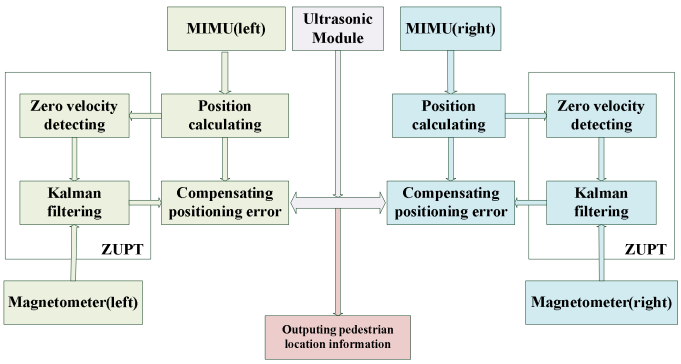

Fig.2 Flow chart of integrated navigation system

Then, the problem of solving the left-foot position can be transformed into a condition of extremum as shown in formula (15).

$$\begin{cases} \breve{x} = \arg\min \left(\mathbf{x}_l - \hat{\mathbf{x}}_l\right)^T \mathbf{W} \left(\mathbf{x}_l - \hat{\mathbf{x}}_l\right) \\ \varphi\left(\mathbf{x}_l\right) = 0 \end{cases} \tag{17}$$

In the form, $\hat{\mathbf{x}}_l$ is the left foot position information calculated by the system and $\hat{\mathbf{x}}_l$ is real left foot position information. $\mathbf{W}$ is weighted matrix.

In general, we consider that:

$$\mathbf{W} = \mathbf{P}^{-1} \tag{18}$$

In the form, $\mathbf{P}^{-1}$ is error covariance matrix of location information.

In the actual situation, the constraint equation can be composed as follows:

$$\varphi\left(\mathbf{x}\right) = \begin{bmatrix} \triangle\mathbf{x}^T & 1 \end{bmatrix} \begin{bmatrix} \mathbf{T} & 0 \\ 0 & C_0 \end{bmatrix} \begin{bmatrix} \triangle\mathbf{x}^T \\ 1 \end{bmatrix} = \triangle\mathbf{x}^T \mathbf{T} \triangle\mathbf{x} + C_0 \tag{19}$$

In the form, there is $\triangle\mathbf{x} = \mathbf{x}_r - \mathbf{x}_l$ and $\mathbf{T}$ is unit matrix.

Then plug in equation (18) and (19) into equation (1), and calculate $\mathbf{x}_l$.

When the pedestrian's left foot touches the ground and the right foot is off the ground, exchange $\mathbf{x}_l$ and $\mathbf{x}_r$. The integrated system needs calculate the left position information by ZUPT and correct right foot position information based on left foot position information. In this way, using the distance $\triangle R$ between the feet as the constraint condition, alternately correct the left and right foot positioning information.

III. PEDESTRIAN NAVIGATION EXPERIMENT

This section we will verify the validity of the pedestrian positioning technology based on MIMU/ magnetometer/ ultrasonic module proposed in the second section, in this section, we will analyze it in detail by indoor pedestrian test. We want to ensure the reliability of the experimental results, so we carry out the experiment of pedestrian location by different paths.

There is the prior knowledge in this paper: the bias of the accelerometer three axes are $0.5\mathrm{m/s}^2$, the drift of the three axes gyroscope three axe are $0.00873^\circ/\mathrm{s}$. The accelerometer three axes noise satisfies the Gauss distribution: $\mathrm{n_a} \sim \mathrm{N}\left(0, 0.001^2\right)$, the gyro three axes noise also satisfies the Gauss distribution: $\mathrm{n_\omega} \sim \mathrm{N}\left(0, 0.000175^2\right)$. The system noise covariance matrix is $\mathbf{Q} = \mathrm{diag}\left(0.5^2\mathbf{I}_{3\times3} \quad 0.00873^2\mathbf{I}_{3\times3} \quad 0.01^2\mathbf{I}_{3\times3}\right)$, and the measurement noise covariance matrix is $\mathbf{R} = \mathrm{diag}\left(0.0001^2\mathbf{I}_{3\times3} \quad 0.0001^2\mathbf{I}_{3\times3} \quad 0.0001^2\mathbf{I}_{3\times3}\right)$. The acceleration threshold of zero velocity detection module is 8500, the angular velocity threshold is 0.1 and the declination is -9°54′.

We carried out pedestrian location experiments at 21 teaching building in Harbin Engineering University. Firstly, we installed the device on the experimenter's feet and preheated for 5 minutes to complete the system initial alignment. Then we have carried out lots experiments and will show three of them. The data collected by the device is stored in a notebook computer through a data line. Finally, the collected data are simulated and analyzed by Matlab. During the test, the experimental installations are fixed in the pedestrian's shoes and the yaw axis are pointing straight ahead of the tester.

Fig. 3 Schematic diagram of device installation

In the first group of experiments, the experimenter went down the hallway to the hall and finally returned to the starting point. The walking distance is about 50 meters, and the time of walking is 2 minutes. The trajectories of pedestrian movements calculated by the combined navigation system are shown as shown in Fig 3. The blue lines represent the trajectory calculated by the integrated navigation system, and the pink lines represent the trajectories calculated by the single inertial navigation system.

From Figure 4 we can see that, the positioning error of the pink lines becomes more and more divergent with time while the starting point and the ending point of the blue line are almost identical. The Euclidean distance between the pink lines is nearly 4m but it is not more than 1m in the blue line. This shows that the integrated navigation system has a significant role in restraining position error and heading error.

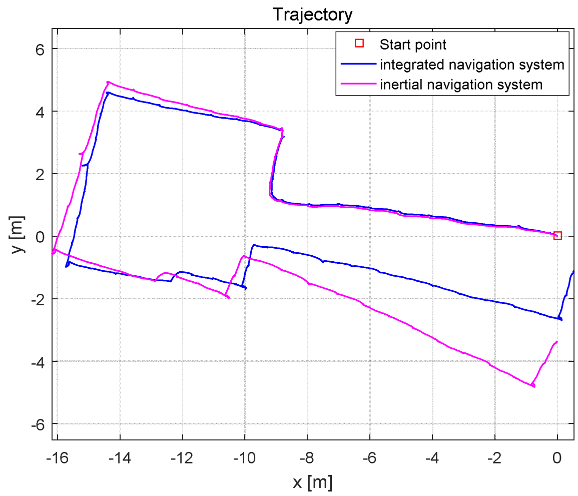

Fig 4. The experimenter trajectories of the first group

In the second group of experiments, the tester went down the hallway to the balcony and then returned to the starting point similarly. The walking distance is about 180 meters, and the time of walking is 5 minutes. The trajectories of pedestrian movements calculated by the integrated navigation system are shown as shown in Fig 5. It can be seen from the diagram that the results of the two navigation systems are distinctly different because of the longer time and distance of the pedestrian movement.

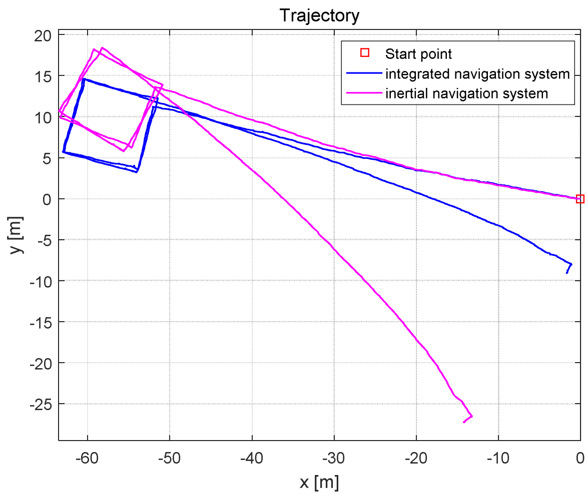

Fig. 5 The experimenter trajectories of the second group

From Figure 5 we can see that, the Euclidean distance between the pink lines is nearly 29.2m but it is not more than 9.1m in the blue line. The presence of the inertial measurement noise makes the positioning accuracy of the inertial navigation system decline with time. But the positioning error of pedestrian positioning system based on dual MIMU/ magnetometer/ ultrasonic module is smaller

In the third group of experiments, the experimenter walked a closed giant in the corridor. The walking distance is about 120 meters, and the time of walking is 3.5 minutes. The trajectories of pedestrian movements calculated by the combined navigation system are shown as shown in Fig 6. The blue lines also represent the trajectory calculated by the integrated navigation system, and the pink lines also represent the trajectories calculated by the single inertial navigation system.

In Figure 6, the blue line shows that the path of a pedestrian is a closed rectangle while the pink line is no longer a real path for pedestrians. The Euclidean distance between the pink lines is nearly 10.05m but it is not more than 1m in the blue line. This shows that the single inertial navigation system cannot fully meet the needs of pedestrians, but the integrated system based on dual MIMU/ magnetometer/ ultrasonic module can achieve better positioning effect.

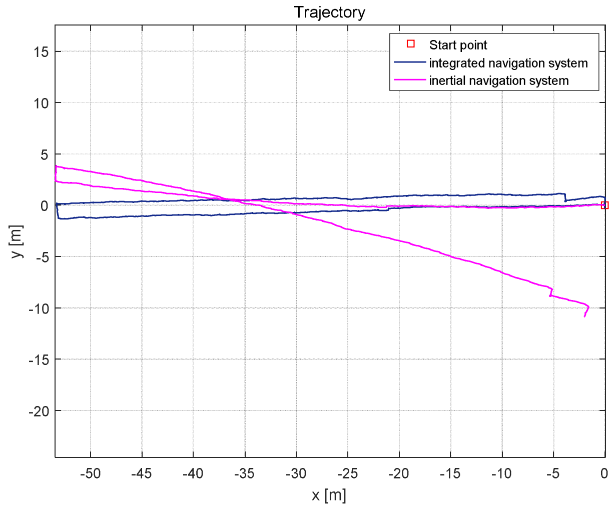

Fig 6. The experimenter trajectories of the third group

From these above experimental results, we can see that the position of the integrated navigation system based on dual MIMU/ magnetometer/ ultrasonic module is basically consistent with the experimental route. Especially the heading error and position error are well suppressed, so the accuracy of pedestrian location is higher.

IV. Conclusion

We processed and analyzed the offline data from the dual MIMU/magnetometer/ultrasonic module positioning system integrated on the foot. The experimental results show that compared with single MIMU pedestrian location technology, pedestrian positioning technology based on dual MIMU/ magnetometer/ ultrasonic module has higher positioning accuracy because it can effectively suppress the heading error and position error. What's more, the positioning accuracy of this integrated system is better in the longer time, which can meet the requirement of pedestrian positioning where there is no external auxiliary information.

Acknowledgment

The paper is funded by the International Exchange Program of Harbin Engineering University for Innovation -oriented Talents Cultivation. And this work is partially supported by National Natural Science Foundation of China (No.51509049), Heilongjiang Science Funds (No.QC2016081), Special Funds for Scientific and Technological Innovation of Harbin (No.2016RAQXJ022), and Heilongjiang Postdoctoral Research Funds (No.LBH-Q16051).

References

[1] Ali A, El-Sheimy N. Low-Cost MEMS-Based Pedestrian Navigation Technique for GPS-Denied Areas[J]. Journal of Sensors, 2013, 2013(4):572-575.

[2] Ojeda L, Borenstein J. Personal dead-reckoning system for GPS-denied environments[C]//Safety, Security and Rescue Robotics, 2007. SSRR 2007. IEEE International Workshop on. IEEE, 2007: 1-6.

[3] Zhao H, Wang Z, Gao Q, et al. Smooth estimation of human foot motion for zero-velocity-update-aided inertial pedestrian navigation system[J]. Sensor Review, 2015, 35(4): 389-400.

[4] Martin H, Groves P, Newman M. The Limits of In‐Run Calibration of MEMS Inertial Sensors and Sensor Arrays[J]. Navigation, 2016, 63(2):127-143.

[5] Yuan X, Liu C, Zhang S, et al. Indoor pedestrian navigation using miniaturized low-cost MEMS inertial measurement units[C]//Position, Location and Navigation Symposium-PLANS 2014, 2014 IEEE/ION. IEEE, 2014: 487-492.

[6] Seco F, Prieto C, Guevara J. A comparison of pedestrian dead-reckoning algorithms using a low-cost MEMS IMU[C]//Intelligent Signal Processing, 2009. WISP 2009. IEEE International Symposium on. IEEE, 2009: 37-42.

[7] Bird J, Arden D. Indoor Navigation With Foot-Mounted Strapdown Inertial Navigation And Magnetic Sensors[J]. IEEE Wireless Communications, 2011, 18(2):28-35.

[8] Aggarwal P, Thomas D, Ojeda L, et al. Map matching and heuristic elimination of gyro drift for personal navigation systems in GPS-denied conditions[J]. Measurement Science & Technology, 2011, 22(2):500-502.

[9] Benzerrouk H, Nebylov A, Salhi H, et al. MEMS IMU/ZUPT Based Cubature Kalman Filter applied to Pedestrian Navigation System[C]//Proceedings of International Electronic Conference on Sensors and Applications. 2014: 1-7.

[10] Ruotsalainen L, Kuusniemi H, Bhuiyan M Z H, et al. A two-dimensional pedestrian navigation solution aided with a visual gyroscope and a visual odometer[J]. Gps Solutions, 2013, 17(4):575-586.

[11] Yang L, Li Y, Rizos C. A WIFI/INS Indoor Pedestrian Navigation System Augmented by Context Feature[C]//China Satellite Navigation Conference (CSNC) 2015 Proceedings: Volume III. Springer Berlin Heidelberg, 2015: 767-780.

[12] Rothman Y, Klein I, Filin S. Analytical Observability Analysis of INS with Vehicle Constraints[J]. Navigation, 2015, 61(3):227-236.

[13] Abdulrahim K, Seman K, Othman M, et al. On magnetometer heading updates for inertial pedestrian navigation system[J]. Gyroscopy and Navigation, 2014, 5(3): 145-152.

[14] Skog I, Händel P, Nilsson J O, et al. Zero-velocity detection—An algorithm evaluation[J]. Biomedical Engineering, IEEE Transactions on, 2010, 57(11): 2657-2666.

[15] Jiménez A R, Seco F, Zampella F, et al. Improved heuristic drift elimination with magnetically-aided dominant directions (MiHDE) for pedestrian navigation in complex buildings[J]. Journal of location based services, 2012, 6(3): 186-210.

[16] Godha S, Lachapelle G. Foot mounted inertial system for pedestrian navigation[J]. Measurement Science & Technology, 2008, 19(7):697-703.

[17] Brand, T. J., & Phillips, R. E. Foot-to-Foot Range Measurement as an Aid to Personal Navigation. Proceedings of the 59th Annual Meeting of The Institute of Navigation and CIGTF 22nd Guidance Test Symposium (2003), 113–121.